

Electronic Supplementary Information (ESI)

Vertical Alignment of Reduced Graphene Oxide/Fe-oxide Hybrids Using the Magneto-Evaporation Method

Sang Cheon Youn, Dae Woo Kim, Seung Bo Yang, Hye Mi Cho, Jae Hyun Lee and Hee-Tae Jung*

Contents :

S1 : Detailed Experiment section

S2: AFM images of graphene oxide

S3 : EDX of GO and RGO/Fe-oxide hybrids

S4 : Raman spectroscopy and XPS data of GO and RGO/Fe-oxide hybrids

S5 : Mechanism of alignment of RGO/Fe-oxide hybrids

S6 : SEM and OM images of stacked graphene sheets

S7 : Effect of metal supporting layer

References of Supplementary Information

S1. Detailed Experiment section

Preparation of graphene oxide : Graphene oxide was prepared using the modified Hummers' method.^[S1] Briefly, a graphite powder (1 g, FP, 99.95% pure, Graphit Kropfuhl AG Inc.) was added to sulfuric acid (98%, 150 ml), which served as a solvent. Then, potassium permanganate (99.0%, 2.5 g), an oxidizing agent, was gradually added to the graphite solution, with vigorous stirring for about 10 min. After allowing the reaction to proceed (at 35°C) for 2 hours, the solution was cooled in an ice bath and diluted with deionized water (200 ml). In the following 4 hours of stirring, hydrogen peroxide (100 ml) was added to the reaction solution. The mixture was then filtrated with a glass filter and washed several times with hydrochloric acid (10%). After this washing process, the remaining solvent was evaporated under vacuum at room temperature for 12 hours.

Fabrication of reduced graphene oxide/Fe-oxide hybrids : We attached a small amount of magnetic nanoparticles, such as iron or iron oxide, onto the GO surface to obtain a system that could be well-aligned by the magnetic fields. This was achieved by means of thermal decomposition.^[S2-4] The iron-oleate complex (as a metal precursor) was prepared by reacting iron chloride and sodium oleate at 70°C and keeping the mixture at that temperature for 4 hours. After completion of the reaction, the solution was cooled to room temperature and the upper organic layer, containing the iron-oleate complex, was washed three times with 30 ml distilled water in a separatory funnel. After washing, hexane was evaporated for 12 hours using a vacuum pump. The iron-oleate complex (12 g) and oleic acid (2.83 g) were dissolved in 1-octadecene (130 ml) at room temperature and then added to GO (150 mg) dispersed in N-methyl-2-pyrrolidone (NMP, 10 ml, with sonication for one hour). The reaction mixture

was heated to 320°C, at a constant heating rate of 1.7°C/min, and then kept at that temperature for 40 min. The resulting solution (containing the nanocrystals) was then cooled to room temperature and ethanol (250 ml) was added to precipitate the GO/Fe-oxide material. In order to separate the product from the unreacted Fe-oxide nanoparticles and obtain only well-dispersed and separated GO solutions lacking flocculated GO particles, the mixture was centrifuged three times, at 6000 g for 30 min, thereby collecting the supernatant solution. We used the vacuum filtration method to obtain the GO/Fe-oxide powder samples. The supernatant solution was subjected to vacuum filtration through a polytetrafluoroethylene (PTFE) membrane with a diameter of 47 mm and a pore size of 500 nm, leading to GO/Fe-oxide samples deposited on the surface of the PTFE membrane. The iron-metal precursors located within the defects of the GO were thermally decomposed, thereby forming Fe-oxide nanoparticles on the surface of the GO. The resulting GO/Fe-oxide samples were dispersed in toluene (<25 mg/L) by means of ultrasonication for 1 hour.

Vertical alignment of RGOs/Fe-oxide hybrids : The resulting solution, containing dispersed GO, was deposited on a substrate such as indium–tin–oxide (ITO) glass or a Si wafer using the dropping method. We positioned a magnet (400 gauss) behind the substrate to apply a magnetic field to the samples. After evaporation of the GO solution in the presence of a magnetic field, we transferred the samples with magnet to a vacuum-evaporator chamber, which operates at a pressure of around 10^{-6} torr. Next, the titanium supporting layer (30 nm), which was used to maintain the vertical alignment of the RGOs, was evaporated from the substrate containing the RGOs. Finally, we removed the samples from the e-beam evaporator and withdrew the magnet, obtaining vertically aligned RGOs on the substrate.

S2. AFM images of graphene oxide

AFM images (and corresponding height profiles) of the GO sheets (**Figure S1**) show that they have lateral dimensions ranging from the submicron to the micron scale and a thickness of about 1.0 nm (**Figure S1b**); this suggests that the GO sheets are comprised of either a single layer or a few layers.^[S5,6] The measured thickness was greater than the theoretical value (0.34 nm) due to the presence of functional groups, such as carboxylic acid, carbonyl, hydroxyl, or epoxy, on the surface and edges of the GO sheets.^[S7]

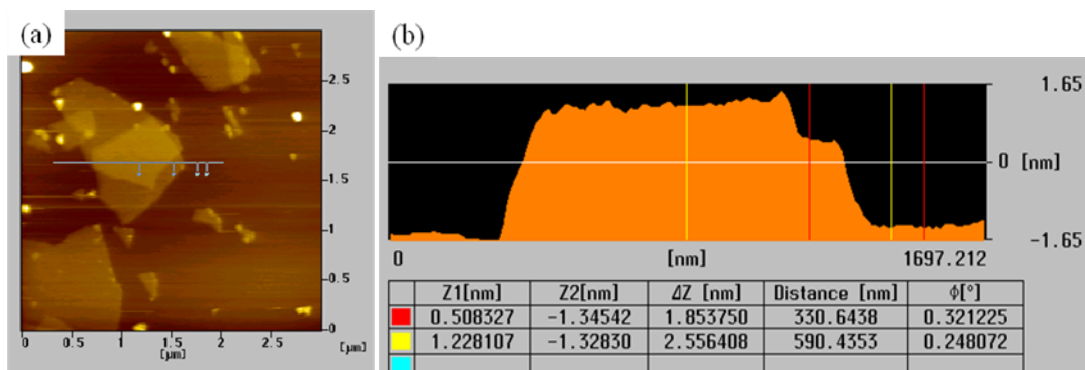


Figure S1. (a) AFM image of the GO which is fabricated by modified Hummers method. (b) The height profiles of GO sheets. The difference of two layers of GO is approximately 0.7 nm.

S3. EDX of GO and RGO/Fe-oxide hybrids

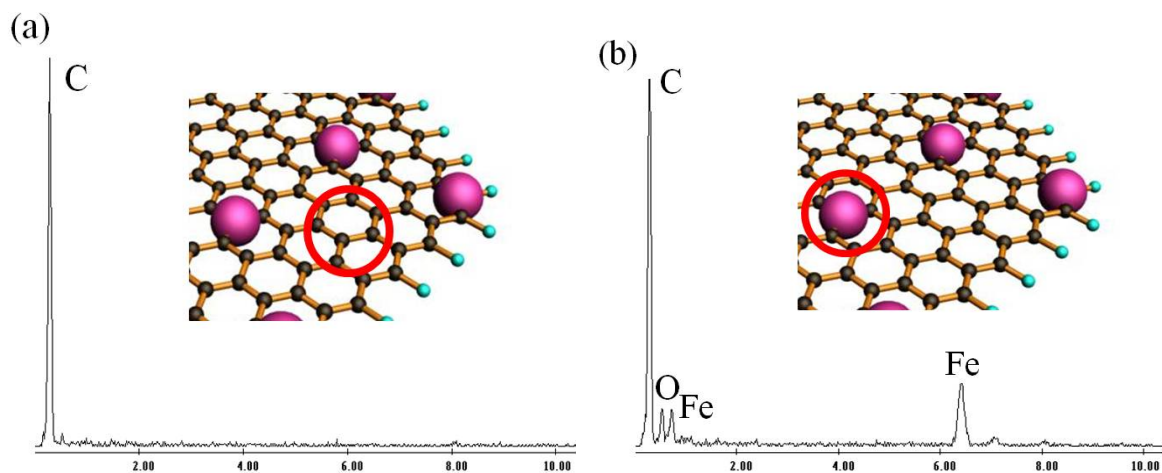
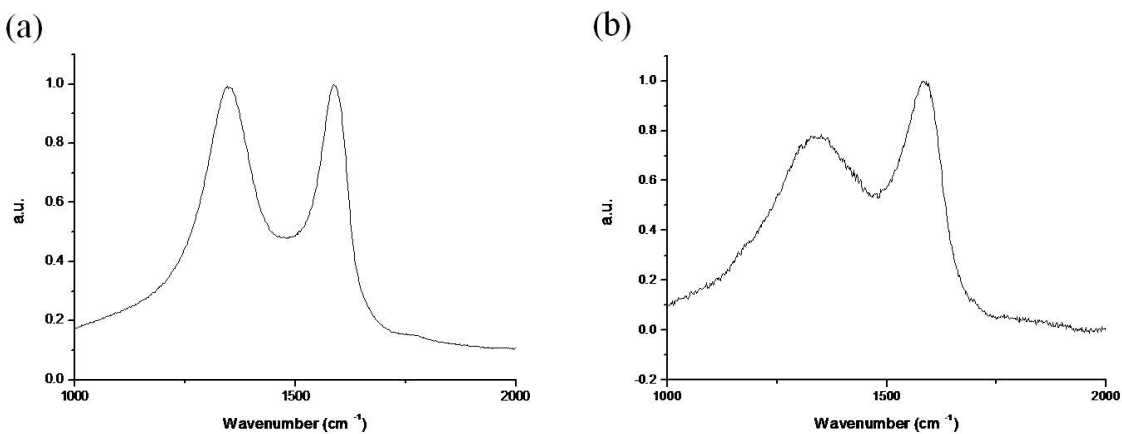


Figure S2. Energy-dispersive X-ray (EDX) results show typical Fe peaks in the range between 6.00 and 7.00 keV, further confirming the presence of Fe-oxide nanoparticles on the GO surface (b), whereas no Fe peaks are detected on that surface (a).

S4. Raman spectroscopy and XPS data of GO and RGO/Fe-oxide hybrids

We found that the resulting GO/Fe-oxide material was effectively reduced during the hybridization of Fe oxide on the GO surface, without using any chemical reducing agents. Dispersive Raman spectroscopy results show that there are two strong bands at about 1580 cm⁻¹ (G band) and 1340 cm⁻¹ (D band) in the first-order spectra of both GO (**Figure S3a**) and GO/Fe oxide (**Figure S3b**), where the G and D bands represent the sp²- and sp³-hybridized carbon–carbon bonds, respectively.^[S8]

Figures S3c and S3d show the C 1s XPS patterns of GO and RGO/Fe-oxide films. GO generated spectra with two dominant peaks at 284.5 and 286.9 eV, corresponding to C–C and C=O species, and two weak peaks at 286.0 and 298.0 eV, corresponding to C–O and O=C–O species (**Figure 3Sc**).^[S9-10] The peaks at 286.0, 286.9 and 289.0 eV indicate the presence of hydroxyl, epoxy, ketone, and carboxylic acid groups on the surface of the GO sheets.



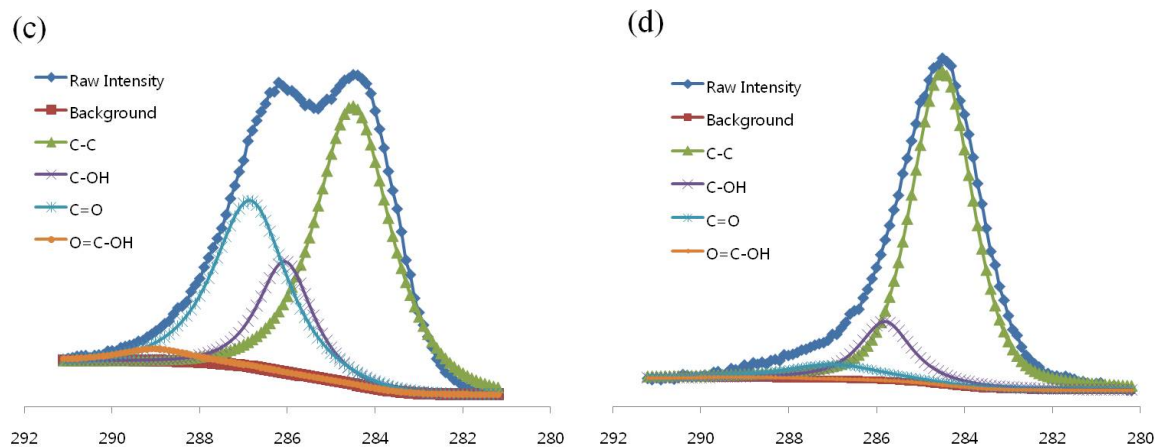


Figure S3. Raman spectroscopy of GO (a) and RGO/Fe-oxide samples (b). The intensity ratio of D-band to G-band is decreased by chemical reaction from 0.99 to 0.75. C(1s) XPS of (c) GO and (d) RGO/Fe-oxide. The peak at 284.5 eV, C-C bonds, becomes more dominant, with the peak corresponding to C=O species becoming weaker with chemical reaction of attachment of magnetic particles.

S5. Mechanism of alignment of RGO/Fe-oxide hybrids



The vector \mathbf{n} indicates the relative position between the moments of metal particles. In this case, the vector \mathbf{n} is parallel the graphene sheets because the metal particles place on the sheet of graphene. When the magnetic field is applied to the RGO/Fe-oxide, the metal particles have a magnetic moment \mathbf{m} and \mathbf{m}' (**Fig S4. (b)**). The magnetic moments of particles is generated to the direction of magnetic field. In this time, the energy is defined by **equation 1**.

The vector \mathbf{B} is also defined by **equation 2**. Under magnetic field, the dipole direction is aligned in the magnetic direction to lower the energy. So, the RGO/Fe-oxide samples is rotated to the magnetic field direction (**Fig S4. (c)**).

$$U = -\mathbf{m} \cdot \mathbf{B} \quad (\text{equation 1.})$$

$$B(m') = -\mu/4\pi d^3 \times [3(\mathbf{n} \cdot \mathbf{m})\mathbf{n} - \mathbf{m}] \quad (\text{equation 2.})$$

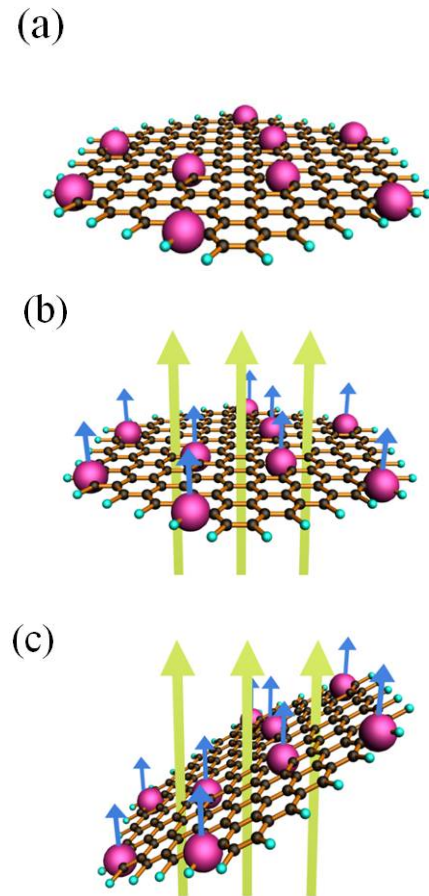


Figure S4. Mechanism of alignment of RGO/Fe-oxide. When the samples were applied by magnetic field, the magnetic particles have magnetic poles (b). Thus, the samples are aligned to the direction of magnetic field because the samples have a lower energy (c).

S6. SEM and OM images of stacked graphene sheets

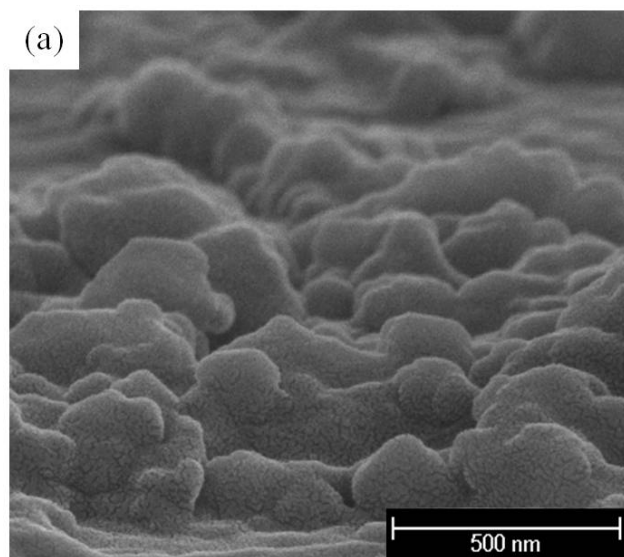


Figure S5. SEM images of vertically aligned stacked graphene sheets using MEA method.

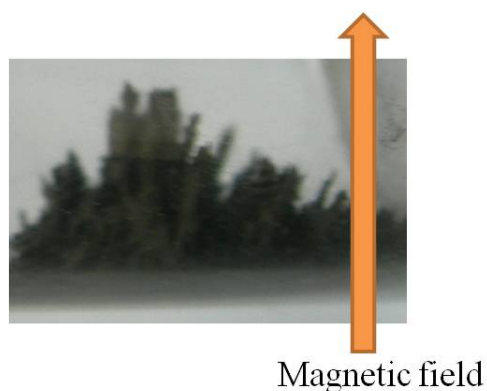


Figure S6. OM images of magnification of Fig 2c. The stacked graphene sheets are aligned to the direction of magnetic field.

S7. Effect of metal supporting layer

The fraction of vertical alignment of the RGOs after titanium evaporation was strongly affected by the thickness of the titanium film. Independently of the titanium evaporation, if a magnetic field was not applied during the process, no vertical alignment occurred (**Figure S7**). Evaporated titanium layers with a thickness below ≈ 20 nm could not sustain the vertical alignment of the RGOs (**Figure S7b**). Upon increasing the thickness of these layers to about 30 nm, most of the RGOs became vertically aligned on the surface. Such vertically aligned RGOs could be observed everywhere on the film after evaporation of the titanium molecules from an approximately 30-nm-thick layer. Our microscopic analysis results show that more than 80% of the RGOs were vertically aligned on the surface. However, this vertical alignment was kept only for thicknesses up to about 100 nm (**Figure S7c**). Titanium layers thicker than that did not produce a sustained vertical alignment, possibly because of the collapse of the vertically aligned RGOs under the weight of the titanium molecules. Thus, the film thickness (≈ 30 nm) of the titanium layer was thoroughly controlled to achieve an optimum alignment of the RGOs over a large area.

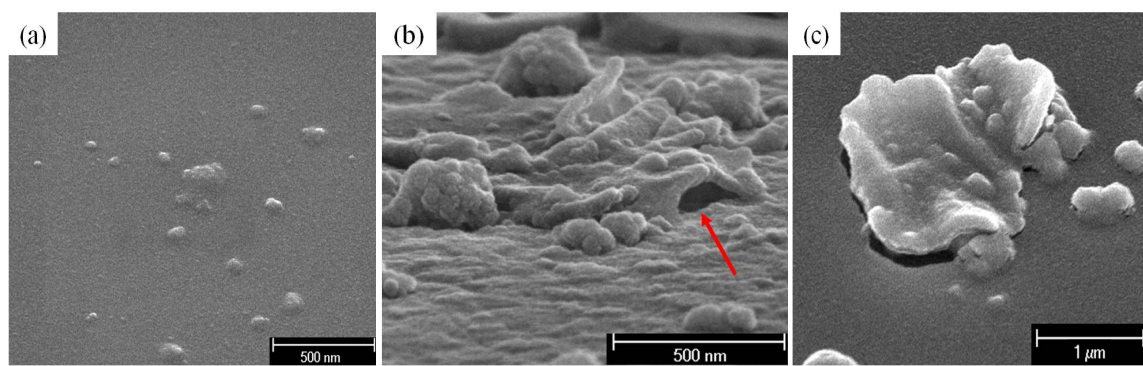


Figure S7. SEM images of non-aligned RGO/Fe-oxide. (a) non-magnetic field with 30nm titanium thickness. (b) 20nm and (c) 100 nm titanium thickness with magnetic field.

References of Supplementary Information

- [S1] M. Hirata, T. Gotou, S. Horiuchi, M. Fujiwara and M. Ohba, *Carbon*, 2004, **42**, 2929-2937.
- [S2] S. C. Youn, D.-H. Jung, Y. K. Ko, Y. W. Jin, J. M. Kim, H.-T. Jung, *J. Am. Chem. Soc.*, 2009, **131**, 742-748.
- [S3] . Park, K. J. An, Y. S. Hwang, J. G. Park, H. J. Noh, J. Y. Kim, J. H. Park, N. M. Hwang and T. Hyeon, *Nat. Mater.*, 2004, **3**, 891-895.
- [S4] J. Park, E. Lee, N. M. Hwang, M. S. Kang, S. C. Kim, Y. Hwang, J. G. Park, H. J. Noh, J. Y. Kini, J. H. Park and T. Hyeon, *Angew. Chem. Int. Ed.*, 2005, **44**, 2872-2877.
- [S5] V. C. Tung, M. J. Allen, Y. Yang and R. B. Kaner, *Nat. Nanotechnol.*, 2009, **4**, 25-29.
- [S6] B. S. Kong, H. W. Yoo and H. T. Jung, *Langmuir*, 2009, **25**, 11008-11013.
- [S7] H. Y. He, J. Klinowski, M. Forster and A. Lerf, *Chem. Phys. Lett.*, 1998, **287**, 53-56.
- [S8] S. Stankovich, D. A. Dikin, R. D. Piner, K. A. Kohlhaas, A. Kleinhammes, Y. Jia, Y. Wu, S. T. Nguyen and R. S. Ruoff, *Carbon*, 2007, **45**, 1558-1565.
- [S9] O. Akhavan, *Carbon*, 2010, **48**, 509-519.
- [S10] J. X. Geng, L. J. Liu, S. B. Yang, S. C. Youn, D. W. Kim, J. S. Lee, J. K. Choi and H. T. Jung, *Journal of Physical Chemistry C*, 2010, **114**, 14433-14440.